INVESTIGATION OF MICROSTRUCTURAL AND MECHANICAL PROPERTIES OF ST-37 AND STRENX-960 STEELS BY A-TIG WELDING METHOD

Emre KASIM[1], Mehmet Fahri SARAÇ[2*], İlyas GENÇ[3]

[1]Süleyman Demirel Üniversitesi, Fen Bilimleri Enstitüsü, Taşıt Teknolojileri ABD, Isparta,
ORCID No: http://orcid.org/0009-0009-9979-8713
[2*]Süleyman Demirel Üniversitesi, Mühendislik ve Doğa Bilimleri Fakültesi, Otomotiv Mühendisliği Bölümü, Isparta,
ORCID No: http://orcid.org/0000-0002-0760-5569
[3]Anka Hidrolik Ürünleri San. Tic. Ltd. Şti., Bursa, ORCID No: http://orcid.org/0009-0000-9287-6795

Keywords

Dissimilar metal welding
A-TIG method
ZrO_2 flux
Al_2O_3 flux
Mechanical properties

Abstract

The place of welding methods in-vehicle technologies is well established, significantly enhancing production speed and product quality. High toughness is crucial for welded metallic structures that require high strength and good processability. However, challenges such as reduced toughness and reliability in welds impact overall quality. This study focused on improving the weld seam quality of dissimilar metals, specifically St-37 and Strenx-960 steels, using the active tungsten inert gas (A-TIG) welding method with ZrO_2 and Al_2O_3 fluxes. Experimental results showed that using ZrO_2 flux yielded the highest mechanical performance, with a hardness of 494.8 HV, tensile strength of 1298 MPa, and impact energy of 113 J/cm². These findings highlight the superior adhesion and crystalline structure of ZrO_2, which minimized defects in the weld seam and HAZ, ensuring consistency in mechanical properties. The study concludes that ZrO_2 flux significantly enhances the mechanical integrity of welded joints, offering potential benefits for vehicle manufacturing.

ST-37 VE STRENX-960 ÇELİKLERİNİN MİKROYAPISAL VE MEKANİK ÖZELLİKLERİNİN A-TIG KAYNAK YÖNTEMİ İLE İNCELENMESİ

Anahtar Kelimeler

Benzer olmayan metal kaynaklama
A-TIG metod
ZrO_2 akısı
Al_2O_3 akısı
Mekanik özellikler

Öz

Kaynak yöntemlerinin taşıt teknolojilerindeki yeri iyi bilinmektedir ve üretim hızını ve ürün kalitesini önemli ölçüde artırmaktadır. Yüksek tokluk, yüksek mukavemet ve iyi işlenebilirlik gerektiren kaynaklı metalik yapılar için çok önemlidir. Ancak, kaynaklarda tokluğun ve güvenilirliğin azalması gibi zorluklar genel kaliteyi etkilemektedir. Bu çalışma, özellikle St-37 ve Strenx-960 çelikleri olmak üzere farklı metallerin kaynak dikişi kalitesini, ZrO_2 ve Al_2O_3 akıları ile aktif tungsten inert gaz (A-TIG) kaynak yöntemini kullanarak iyileştirmeye odaklanmıştır. Deneysel sonuçlar, ZrO_2 akısının kullanılmasının 494,8 HV sertlik, 1298 MPa çekme dayanımı ve 113 J/cm² darbe enerjisi ile en yüksek mekanik performansı sağladığını göstermiştir. Bu bulgular, kaynak dikişindeki ve Isının Tesiri Altındaki Bölge (ITAB)'de ki kusurları en aza indirerek mekanik özelliklerde tutarlılığı sağlayan ZrO_2'nin üstün yapışma özelliğini ve kristal yapısını vurgulamaktadır. Çalışma, ZrO_2 akısının kaynaklı bağlantıların mekanik bütünlüğünü önemli ölçüde artırdığı ve araç üretimi için potansiyel faydalar sağladığı sonucuna varmıştır.

Araştırma Makalesi		Research Article	
Başvuru Tarihi	: 02.09.2024	Submission Date	: 02.09.2024
Kabul Tarihi	: 23.01.2025	Accepted Date	: 23.01.2025

* Sorumlu yazar: fahrisarac@sdu.edu.tr
https://doi.org/10.31796/ogummf.1542071

1. Introduction

Welding joints play a critical role in various industrial sectors, including shipbuilding, pressure vessel manufacturing, railways, crane production, and agriculture (Korkmaz, Çetin, Adar, and Orak, 2020; Vidyarthy and Sivateja, 2020; Singh and Khanna, 2021). The process of welding joins two metals, whether similar or dissimilar, using heat and/or pressure, and the most common methods include submerged arc, gas-submerged arc (TIG, MIG, and MAG). These methods allow joining parts that experience significant mechanical stresses in their applications using high-strength materials (Akgün, Buran and Sarac, 2023;

Vidyarthy and Dwivedi, 2016; Sharma and Dwivedi, 2021a). However, using high-strength materials can increase production costs and present challenges in material acquisition.

Steels are widely used in industries ranging from construction to healthcare due to their availability, cost-effectiveness, and customizable mechanical properties achieved through alloying and heat treatment. The combination of different steel types is essential in applications where a balance of mechanical properties, such as strength, wear resistance, and workability, is needed (e.g., in machine elements and structural components). However, joining different steels poses challenges, including potential welding defects such as pores, insufficient melting, penetration issues, distortion, axial misalignment, cracks, and weld foaming (Vijay, Mohanasundaram, Ramkumar, Kim, Tugriumubano, and Go, 2020; Sharma and Dwivedi, 2021b).

Examples of alloy sources used were examined to prevent the increase in costs. In the study of İpekoğlu, Küçükömeroğlu, Aktarer, Sekban, and Çam (2018), the mechanical properties and changes in the microstructure of St-37/St52 different low carbon steels were investigated by friction stir welding (FSW) welding method, while Kulkarni, Dwivwdi and Vasudevan (2018) investigated the effects of different steel combinations consisting of 8 mm thick sheets of modified 9Cr-1Mo (P91) steel and 2.25Cr-1Mo (P22) steel welded by active flux TIG welding method on the weld seam geometry under different gas flows such as SiO_2, TiO_2, Cr_2O_3, MoO_3 and CuO, and the integrity of the weld joint made with MoO_3 flux, metallurgical and mechanical properties after welded and post-weld heat treatment (750°C and 2 hours) method. Adar (2019) investigated the weldability of Hardox-500 and St-52 steels by robotic arc welding method at different current and voltage values. Ahola, Lipiäinen, Riski, Koskimaki, Pyörret, and Björk (2023) compared the fatigue strength improvement of shot peened and clean blast welded joints by considering butt welded and fillet welded components, fatigue tests of joints under post-weld process conditions on TIG clad and HFMI processed S355, S700 and S1100 fillet welded specimens in their study. Güzey and Irsel (2023) investigated the microstructural and mechanical aspects of joining high-temperature and pressure-resistant P355GH and austenitic stainless 316L steels by the Tungsten Inert Gas (TIG) welding method.

The motivation for combining St-37, a general-purpose low-carbon steel, with Strenx-960, a high-strength structural steel, lies in leveraging the complementary properties of these materials. St-37 offers good ductility and ease of processing, while Strenx-960 provides exceptional strength and toughness. Combining these steels aims to achieve a weld joint that balances ductility and strength, meeting the stringent requirements of various industrial applications. Despite the potential advantages, no comprehensive study has examined welded joints' microstructural and mechanical behaviour between Strenx-960 and St-37 using A-TIG welding with ZrO_2 and Al_2O_3 fluxes (Teker, Yılmaz ve Karakurt, 2018; Tümer, Mert and Karahan, 2020; Aras and Ertan, 2024). This study seeks to fill that gap, focusing on how these fluxes influence weld quality, mechanical performance, and structural properties.

The use of metal oxide powders such as ZrO_2 and Al_2O_3 in A-TIG welding has been shown to enhance penetration depth, minimize distortion, and improve overall weld quality. These materials were selected due to their high adhesion and crystalline structures, contributing to superior mechanical properties in the welded joint (Vidyarthy and Dwivedi, 2016; Singh and Khanna, 2021; Afzali and Asghari, 2022). This study aims to determine the impact of ZrO_2 and Al_2O_3 fluxes on the weld zone mechanics and structure of Strenx-960 and St-37, thus providing valuable insights for industrial applications that demand high-quality welded joints.

2. Material and methods

2.1. Material

Heray Filtration and Water Technologies Inc. provided Strenx-960 and St-37 materials, each 8 mm thick. Additionally, Al_2O_3 and ZrO_2 metal oxide powders of sub-1 micron size were purchased from Sigma Aldrich. The chemical compositions of the materials provided by the supplier are outlined in Table 1. Each plate to be welded was 100 mm × 100 mm × 8 mm.

Table 1. Chemical Composition (in wt. %)

	Fe	C	Si	Mn	P	S	Al
St-37	Bal.	0.11	0.03	0.56	0.01	0.01	-
Strenx -960	Bal.	0.18	0.5	1.7	0.02	0.01	0.02

2.2. Welding Step

The surfaces of St-37 and Strenx-960 steels were smoothed using 800 mesh sandpaper. Sub-1 micron 10-gram weight Al_2O_3 and ZrO_2 powders were mixed with 32 ml of ethanol and then applied to the welding interface. The welding process was initiated after the ethanol evaporated for 1 hour.

The welding parameters were set as follows: 2 mm arc height, 4 mm/s arc speed, and welding current values of 120A and 160A (Singh and Khanna, 2021). Two plates were prepared for each parameter set and classified according to the test parameters in Table 2, which provides details of the test samples' classification.

Table 2. Sample Classifications

Sample Code	A-TIG Procedure	Welding Current
A	No flux	120A
B	No flux	160A
C	ZrO_2 flux	120A
D	ZrO_2 flux	160A
E	Al_2O_3 flux	120A
F	Al_2O_3 flux	160A

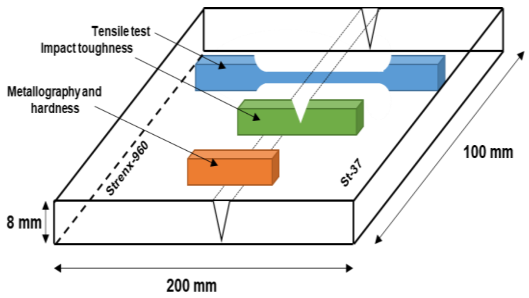

(a)

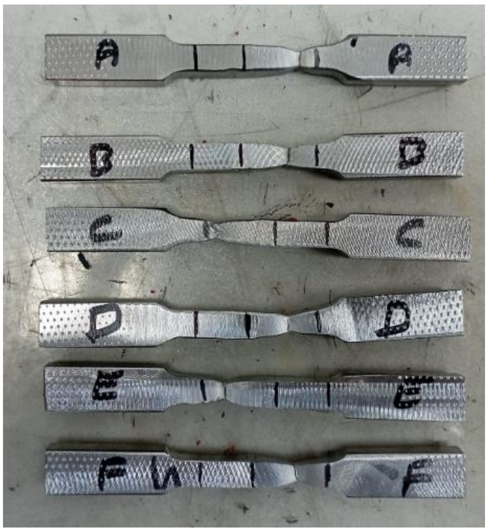

(b)

Figure 1. (a) Dimensions of Test Samples to be Cut with a Water Jet, (b) Prepared Samples for Tensile Test.

2.3. Characterization

All samples were subjected to standard metallographic procedures, including grinding (80 mesh to 1200 mesh), polishing, and etching. Both stereo (Zeiss Stemi 508 model) and optical (Olympus BX51TRF-6 model) microscopes captured images of the weld area and surrounding grain structures.

The mechanical properties of the weld region were evaluated through microhardness, tensile, and Charpy impact toughness analyses. Vickers microhardness was measured on the weld cross-section using a 200 g load for a 10-second dwell time, following the ASTM E92-16 standard. Measurements were taken at 10 mm intervals using a microhardness tester (VH1 MD, Make: Chennai Metco Economet). Each sample was tested at five points, and an average value was calculated to compare them. Tensile tests were operated on transverse weld specimens prepared according to ASTM E-8 standard using an INSTRON 5980 tensile testing machine at a 1 mm/min speed. The Charpy impact toughness test was performed on specimens with dimensions of 55 mm × 10 mm × 5 mm with a V-notch machined in the middle of the sample according to the ASTM E370 standard. Five samples were prepared for each tensile and Charpy impact toughness test measurement set. Scanning electron microscopy (SEM) was used to analyze the fractured surfaces and investigate the fracture modes during the tensile tests. This study complies with research and publication ethics.

3. Results

The stereo-microscope images in Figure 2 show the entire weld area of each sample. It was observed that the weld connection of the samples without flux and with Al_2O_3 flux was not sufficiently formed, resulting in weld gaps (weld groove, colored with blue circle). This was likely due to insufficient welding current. Conversely, the weld connection of the ZrO_2 flux sample showed no surface defects. Furthermore, the HAZ region exhibited a homogeneous and flawless internal structure.

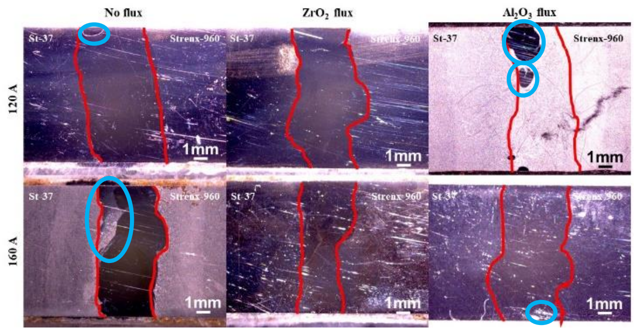

Figure 2. The Stereomicroscope Images Show the Welding Region Located Between The Two Red Lines

In Figure 3, the optical microscope images of Strenx960, St-37, and the HAZ region show that the internal structure of the St-37 material has a tightly lamellar pearlite phase. On the other hand, the Strenx-960 material displays the presence of the martensite structure. Despite similar internal structures in all samples, the distinct mechanical properties of both materials clearly and decisively differentiate the transition line.

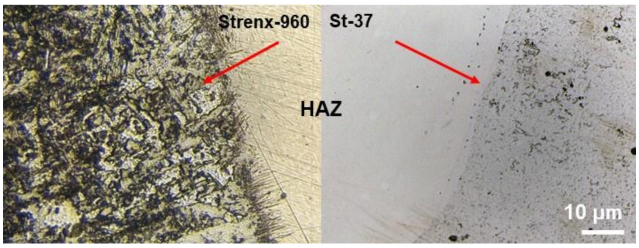

Figure 3. Optical Microscope Images of Strenx-960 and St-37 After Welding

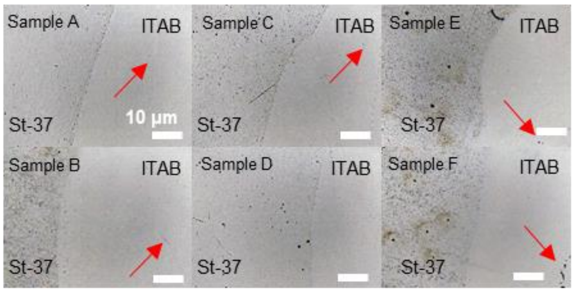

Figure 4. Optical Microscope Images of All Samples Showing Welding Grooves

Figure 4 presents optical microscope images of the welding transition zones across all samples. The weld grooves are indicated as points in the areas marked by the red arrows. Each sample was imaged at the same magnification, with a scale bar of 10 µm accompanying each image. A closer examination reveals that the transition zones from the weld area to the St-37 material are clearly defined. Particularly noteworthy is the flawless surface formation observed in Sample D.

In Figure 5, hardness values were measured at five different horizontal points of each sample. During each measurement, hardness values were taken from 5 points perpendicular to the determined point, and average hardness values were calculated. Standard deviation is less than 10 HV for each set of samples. Upon examining the hardness test measurement results, it was observed that both St-37 (310 HV) and Strenx-960 (360 HV) had higher average hardness values than the weld area. This is contrary to the general expectation in the literature, which suggests that the hardness of the weld area would be higher than that of two different metals. However, in this study, the region's toughness value decrease can be explained by the high hardness values of both main materials and the high heat input to the weld area (Adar, M., 2019).

Furthermore, when the graph is examined, it is evident that hardness significantly decreases in the absence of flux materials. In contrast, the hardness values improve or increase in the presence of Al_2O_3 and ZrO_2 flux materials, respectively. This observation indicates a direct relationship between the internal structure and the adhesion effect (Afzali and Asghari, 2022).

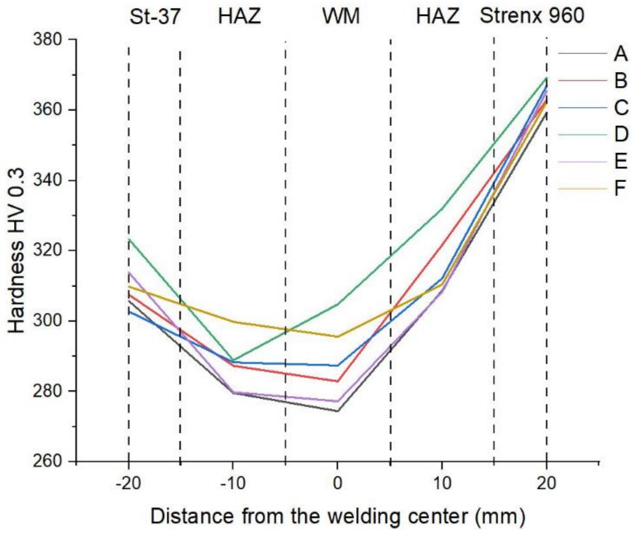

Figure 5. The Vickers Microhardness Measurement (HV 0.3) Demonstrates the Variance in Hardness Throughout the Welding Zone.

Five different materials were prepared from each set of samples in the tensile, and Charpy impact tests were performed on all samples. The average values of the experiment involved preparing five different materials from each set of samples for tensile and Charpy impact tests. The average values of the measurements were calculated and shown in Figure 6. Upon examining the results of the tests, it was noted that the values were very similar. It was observed in all experiments that the deformation occurred within the weld and heat-affected zone (HAZ) region. This suggests that the weld seam quality was consistent across all samples. However, it was also noted that the mechanical properties of the ZrO_2 fluxed materials exhibited a more ductile behavior than the other samples.

In particular, the impact energy increased from 60J/cm^2 to 113J/cm^2, and the tensile strength increased by 40MPa compared to the non-flux welded materials. The measurements were calculated and shown in Figure 6. When the results of the tensile and Charpy tests were examined, it was seen that the values were very close to each other. In all experiments, it was determined that the deformation occurred within the weld and HAZ region. This situation shows that the weld seam quality was obtained at similar values in each sample. However, it can still be said that the mechanical properties of ZrO_2 fluxed materials exhibited a more ductile behavior compared to other samples. Especially when compared to no flux welded materials, it was observed that the impact energy increased from 60J/cm^2 to 113J/cm^2, and the tensile strength increased by 40MPa.

Moreover, the observed low percentage elongation values in Samples A, B, and E can be primarily linked to factors that affect the mechanical properties of the welded joints. Samples A and B were subjected to welding processes that did not utilize any flux material. This omission may have resulted in inadequate adhesion in the weld region, leading to the development of defects such as pores. While Sample E employed Al_2O_3 flux, the strong adhesion afforded by ZrO_2, coupled with the absence of a crystal structure, may have adversely affected the mechanical integrity of the weld bead. In the cases of Samples A and B, the lack of flux contributed to reductions in hardness and strength within the weld area, ultimately resulting in low elongation values. Additionally, the effectiveness of Al_2O_3 flux in Sample E was inferior to that of ZrO_2, which explains the persistently lower percentage elongation values compared to the other samples. This phenomenon can be attributed to the distinct structural properties of the various fluxes and their respective impacts on the weld area.

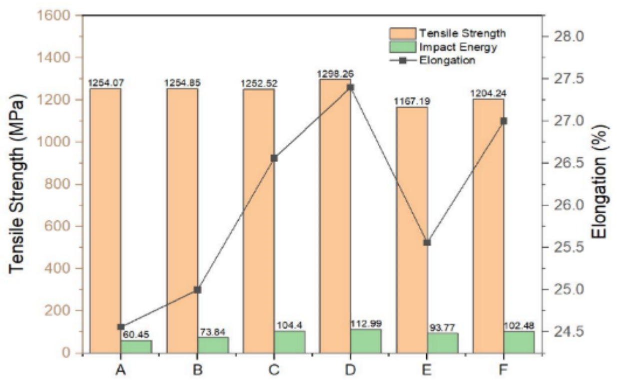

Figure 6. Mechanical Properties (Tensile and Charpy Impact) of All Samples After the Welding Process

In Figure 7, SEM was used to capture cross-sectional area images of the fracture surfaces following the tensile test at 3000x magnification for 10μm. A typical ductile shear fracture mechanism exhibits a cup-and-cone fracture morphology when examining the images. The pattern and size distribution of the pits on the fracture surface are related to the distribution of martensite particles. The minor smooth background on the No-flux fracture surfaces reflects the void nucleation in the fibrous martensite structures (Avramovic-Cingara, Saleh, Jain and Wilkinson, 2009). The different pit sizes seen in the ZrO_2 and Al_2O_3 flux samples reveal the deformation of the ferrite at the final stress moment. This observation caused several large voids due to the significant plastic deformation of the sample before rupture.

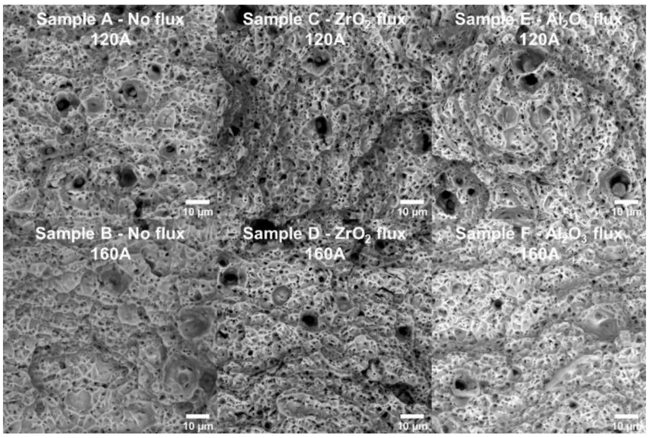

Figure 7. Cross-section Image of Fractured Surfaces on the Welding Zone for All Samples After Tensile Test

4. Conclusions

This study comprehensively investigated the welding of high-strength and high-hardness structural steel Strenx-960 and low-carbon general-purpose steel St-37 using different flux materials (ZrO_2 and Al_2O_3) and variable current conditions using the A-TIG welding method.

When ZrO_2 flux was used with 160A welding current, the average tensile strength was measured as 1298 MPa, impact strength as 113 J/cm^2, and hardness as 494.8 HV. These results provided the highest mechanical performance compared to other samples and revealed the positive effect of ZrO_2 flux on weld quality. The high adhesion and crystal structure of ZrO_2 minimized the defects in the weld bead and heat-affected zone (HAZ). They increased the homogeneity in the microstructure, thus ensuring consistent mechanical properties. In welding processes using Al_2O_3 flux, tensile strength remained around 1220 MPa and impact strength around 85 J/cm^2. Although these values were lower than ZrO_2, they provided better results than those without flux. This situation shows the limited effect of the crystal and adhesion properties of Al_2O_3. Samples without flux (A and B) showed low values , such as tensile strength of 1100 MPa and impact strength of 60 J/cm^2. This situation shows that insufficient adhesion and welding defects occurred in the weld area due to the lack of flux and insufficient mechanical properties. These qualitative differences observed in the samples using flux emphasize the importance of selecting the suitable flux material to obtain the desired welding properties. ZrO_2 flux has effectively created durable welded joints that can be used in the automotive and heavy machinery industries, primarily by increasing mechanical properties such as ductility and toughness.

In conclusion, using ZrO_2 flux in the A-TIG welding process significantly improved the mechanical and microstructural quality of welds between St-37 and Strenx-960 steels. These findings provide practical information for projects requiring robust, high-performance welded joints in industrial applications.

Acknowledgments

This work was financially supported by the Scientific Research Fund for the Suleyman Demirel University (FYL-2024-9283). The authors are grateful for all this support.

Contributions of the Researchers

In this study, Emre KASIM contributed to the literature review, methodology, test analysis, and manuscript writing; Mehmet Fahri SARAÇ contributed to the conceptualization, manuscript writing, revision, and data evaluation; and İlyas GENÇ contributed to test execution and material procurement.

Conflict of Interest

The authors have no competing interests relevant to this article's content.

References

Adar, M. (2019). Investigation of Weldability of Hardox-500 and St-52 Steel by Mechanical Tests and Statistical Methods, Karabük University, Graduate School of Natural and Applied Sciences, Department of Mechanical Engineering, M.Sc. Thesis, September 2019, Karabük.

Afzali, M., and Asghari, V. (2022). Study of the effect of nano ZrO_2 and TiO_2 and rotation speed on friction behavior of rotary friction welding of HIPS and PP, *Functional Composites and Structures,* 4, 015002. https://doi.org/10.1088/2631-6331/ac407d

Ahola, A., Lipiäinen, K., Riski, J., Koskimaki, M., Pyörret, J., Björk, T. (2023). Fatigue Strength Of Shot-Peened As-Welded Joints And Post-Weld-Treated And Subsequently Clean-Blasted Fillet Weld Joints, *Welding in the World*, 67, 1559–1574. https://doi.org/10.1007/s40194-023-01498-3

Akgün, G., Buran, D., Sarac, M.F. (2023). Investigation of Microstructure and Wear Behaviors of AZ91 Alloy Under Different Heat Treatment, *Erzincan University Journal of Science and Technology*, 16, 516-527. https://doi.org/10.18185/erzifbed.1254273

Aras, S. and Ertan, R. (2024). Studying the Strength of Dissimilar Joints of AISI 430 and 301 Stainless Steel Welded at Different Welding Parameters, *Materials and Technology*, 58, 121-127. https://doi.org/10.17222/mit.2023.1054

Avramovic-Cingara, G., Saleh, Ch.A.R., Jain, M.K., Wilkinson, D.S. (2009). Void Nucleation and Growth in Dual-Phase Steel 600 during Uniaxial Tensile Testing, *Metallurgical and Materials Transactions A*, 40, 3117-3127. https://doi.org/10.1007/s11661-009-0030-z

Güzey, B.N. and Irsel, G. (2023). Investigation of Mechanical and Microstructural Properties in Joining Dissimilar P355GH and Stainless 316L Steels by TIG Welding Process, *International Journal of Pressure Vessels and Piping*, 205, 104965. https://doi.org/10.1016/j.ijpvp.2023.104965

İpekoğlu, G., Küçükömeroğlu, T., Aktarer, S.M., Sekban, D.M., Çam, G. (2019). Investigation of microstructure and mechanical properties of friction stir welded dissimilar St37/St52 joints, *Materials Research Express*, 6, 046537. https://doi.org/10.1088/2053-1591/aafb9f

Korkmaz, Ş., Çetin, M.H., Adar, M., Orak, A. (2020). Investigation of Tensile Strength and Hardness Behaviour of Hardox500 – St52 Specimen Joined by GMAW Method, K*onya Journal of Engineering Sciences*, 8 (2), 300-317. https://doi.org/10.36306/konjes.610889

Kulkarni, A., Dwivedi, D.K., Vasudevan, M. (2018). Study Of Mechanism, Microstructure And Mechanical Properties Of Activated Flux TIG Welded P91 Steel-P22 Steel Dissimilar Metal Joint, *Materials Science And Engineering*: A, 731, 309-323. https://doi.org/10.1016/j.msea.2018.06.054

Sharma, P. and Dwivedi, D.K. (2021a). A-TIG welding of dissimilar P92 steel and 304H austenitic stainless steel: Mechanisms, microstructure and mechanical properties, *Journal of Manufacturing Processes*, 44, 166-178.

https://doi.org/10.1016/j.jmapro.2019.06.003

Sharma, P. and Dwivedi, D.K. (2021b). Wire-feed Assisted A-TIG Welding of Dissimilar Steels, *Archives of Civil and Mechanical Engineering*, 21, 81. https://doi.org/10.1007/s43452-021-00235-1

Singh, S.R., Khanna, P. (2021). A-TIG (activated flux tungsten inert gas) welding:- A review, *Materials Today: Proceedings*, 44(1), 808-820. https://doi.org/10.1016/j.matpr.2020.10.712

Teker, T., Yılmaz, S.O., Karakurt, E.M. (2018). Effect of different rotational speeds on mechanical and metallurgical properties of friction welded dissimilar steels, *Materials Testing,* 60, 135-141. https://doi.org/10.3139/120.111135

Tümer, M., Mert, T., Karahan, T. (2020). Investigation of microstructure, mechanical, and corrosion behavior of nickel-based alloy 625/duplex stainless steel UNS

S32205 dissimilar weldments using ERNiCrMo-3 filler metal, *Welding in the World,* 65, 171-182. https://doi.org/10.1007/s40194-020-01011-0

Vidyarthy, R.S. and Dwivedi, D.K. (2016). Activating flux tungsten inert gas welding for enhanced weld penetration, *Journal of Manufacturing Processes*, 22, 211-228. https://doi.org/10.1016/j.jmapro.2016.03.012

Vidyarthy, R.S. and Sivateja, P. (2020). Influence of activating flux tungsten inert gas welding on mechanical and metallurgical properties of the mild steel, *Materials Today: Proceedings*, 28(2), 977-981. https://doi.org/10.1016/j.matpr.2019.12.33

Vijay, S.J., Mohanasundaram, S., Ramkumar, P., Kim, H.G., Tugriumubano, A., Go, S.H. (2020). Experimental Investigations on Activated-TIG Welding of Inconel 625 and AISI 304 Alloys, *Advances in Materials and Manufacturing Engineering*, 311–317. https://doi.org/10.1007/978-981-15-1307-7_34